Exploration of resonance properties in chiral perturbation theory with explicit $U_A(1)$ anomaly

Zhi-Hui Guo[a,b] and J. A. Oller[b]

[a]*Department of Physics, Hebei Normal University, 050016 Shijiazhuang, China*
[b]*Departamento de Física, Universidad de Murcia, E-30071 Murcia, Spain*

We study the resonance properties within chiral perturbation theory by explicitly taking into account the $U_A(1)$ anomaly effect. This assures we have the appropriate degrees of freedom of low energy QCD in the large N_C limit. We calculate the various resonance properties, such as mass, width and residues, for the physical case, i.e. $N_C = 3$. Then we extrapolate the values of N_C to study the trajectories of resonance poles.

1 Introduction

The combination of chiral perturbation theory (χPT) and non-perturbative methods inspired from S- matrix theory, play an important role in the study of resonances nowadays [1]. A straightforward application of this approach is to determine the properties of the resonance, such as the mass and the width. A deeper understanding of the resonance structure can be obtained by combining the $1/N_C$ expansion of QCD in χPT [2]. A novel ingredient in our current study is the singlet η_1, which is massive even in the chiral limit due to the $U_A(1)$ anomaly effect. This ingredient has been commonly ignored in the previous works on the study of N_C trajectories of resonance poles [2]. Since it turns out to be the ninth pseudo Goldstone in the chiral and large N_C limit and becomes a relevant degree of freedom in the low energy QCD for large N_C, it is necessary to take this effect into account to study resonance properties at large N_C. In our study, this gap is filled by using the $U(3)$ χPT, which incorporates the massive singlet η_1 as its explicit degree of freedom.

2 Theoretical setup

The current study of resonance properties is based on the complete one-loop calculation of meson-meson scattering within $U(3)$ χPT by explicitly including the tree level exchanges of scalar and vector resonances. The perturbative calculation incorporates not only the genuine meson-meson scattering diagrams, including the loops and the resonance exchanges, but also the contributions from the wave function renormalizations, mass renormalizations,

pseudo-Goldstone weak decay constants and $\eta - \eta'$ mixing. The master formula to unitarize the perturbative $U(3)$ χPT results is from a simplified version of N/D method derived in [3]

$$\text{(1)} \qquad T_J^I(s)^{-1} = N_J^I(s)^{-1} + g(s) \,,$$

where $T_J^I(s)$ denotes the unitarized partial wave amplitudes with well defined isospin I and angular momentum J. $N_J^I(s)$ collects the crossed channel cuts and can be constructed from the perturbative results

$$\text{(2)} \qquad N_J^I(s) = T_J^I(s)^{(2)+\text{Res}+\text{Loop}} + T_J^I(s)^{(2)} \, g(s) \, T_J^I(s)^{(2)} \,,$$

where $T_J^I(s)^{(2)+\text{Res}+\text{Loop}}$ stands for the partial wave amplitude from the perturbative calculation, with the superscripts (2), Res and Loop denoting the leading order amplitudes, resonance exchanges and loop contributions, respectively. The explicit expressions from the perturbative calculation can be found in Ref. [4]. $g(s)$ contains the right hand cuts and its explicit expression can be also found in [4] and references therein.

3   Results and Discussions

From the unitarized meson-meson scattering amplitudes, one can construct the phase shift, modulus of the S-matrix and invariant mass distribution [4]. Then we fit the various quantities to the experimental data to get the unknown parameters in our model. The resonance poles are found on the unphysical Riemann sheets, which can be obtained from the extrapolation of T-matrix on the physical sheet (the first sheet) to the unphyscial ones. In our study, the pole positions of three kinds of vector resonances are obtained: $\rho(770)$ with $IJ = 1\,1$, $K^*(892)$ with $IJ = \frac{1}{2}\,1$ and $\phi(1020)$ with $IJ = 0\,1$. For the scalar resonances, we find σ, $f_0(980)$ and $f_0(1370)$ for the $IJ = 0\,0$ case, $a_0(980)$ and $a_0(1450)$ for $IJ = 1\,0$ case, κ and $K^*(1430)$ for $IJ = \frac{1}{2}\,0$. The masses and widths of the above mentioned resonances are consistent with the PDG values [5]. We have also calculated the couplings between the resonances and the pseudo-scalar mesons. For the detailed result, see Ref. [4].

Then we extrapolate the values of N_C from 3 to larger numbers to study the corresponding behaviors of resonance poles. In this way, one can learn whether the resonance is a standard $\bar{q}q$ resonance by plotting the N_C trajectories of its pole positions. The basic criteria is that in the framework of large N_C QCD the mass of a standard $\bar{q}q$ resonance is a constant, while its decay width decreases as $1/N_C$ when N_C approaches to infinity. For $\rho(770)$, $K^*(892)$, $f_0(980)$, $f_0(1370)$, $a_0(1450)$ and $K^*(1430)$, we plot the quantities of $\Gamma * N_C$ (Γ denotes the width) and mass of the resonances as functions of N_C in Figs. 1 and 2 respectively. It is clear that the resonances appearing in those two figures all behave as the standard $\bar{q}q$ resonances, since their masses are more or less stable when varying N_C and their decay widths decrease as $1/N_C$ for large values of N_C. However for the very broad resonances σ and κ, we find their pole positions in the complex s plane approach to the real and negative axis when
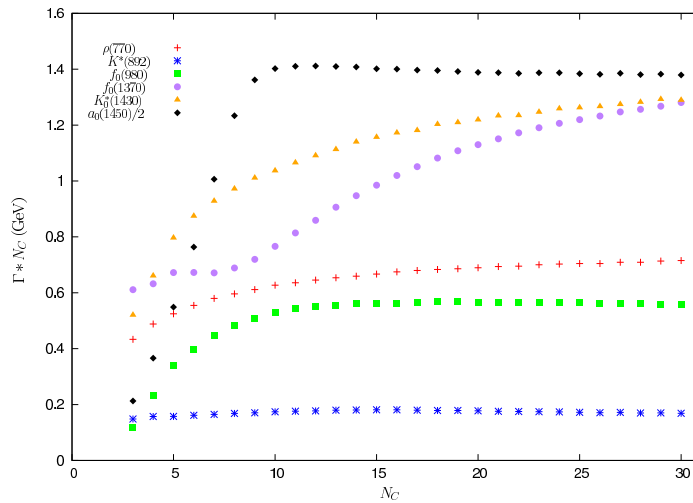
Figure 1: Decay widths of resonances as functions of N_C. For $a_0(1450)$, we plot the quantity of $\Gamma * N_C/2$. For the others, we plot the quantity of $\Gamma * N_C$ as functions of N_C.

increasing the values of N_C. In this case, it is not appropriate to interpret the imaginary part of $\sqrt{s}$ as the decay width. In Fig. 3, we plot the real and imaginary parts of s_σ and s_κ as functions of N_C, from where one can conclude that σ and κ resonances in our study do not correspond to the standard $\bar{q}q$ resonances for large N_C. For $a_0(980)$, both its width and mass increase when increasing N_C, indicating it does not seem to correspond to a standard $\bar{q}q$ resonance in our current study.

Acknowledgments

References

[1] J. Oller and E. Oset, Nucl. Phys. **A620** (1997) 438; (E)−*ibid* A **652**(1999) 407; M. Albaladejo and J. A. Oller, Phys. Rev. Lett. **101** (2008) 252002; I. Caprini, G. Colangelo and H. Leutwyler, Phys. Rev. Lett. **96** (2006) 132001.
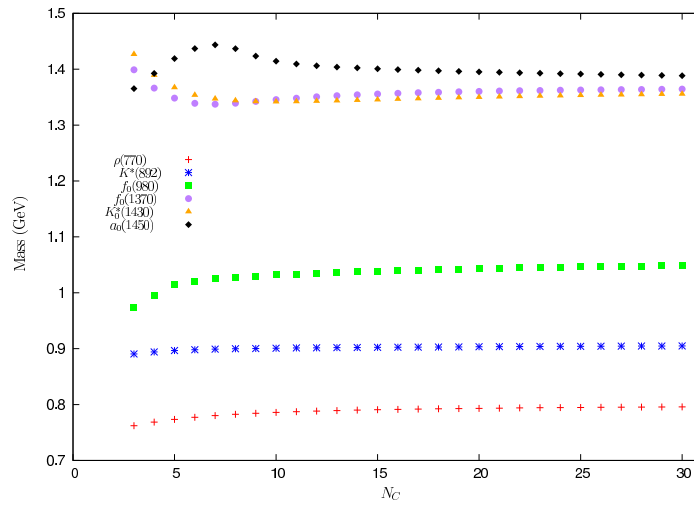
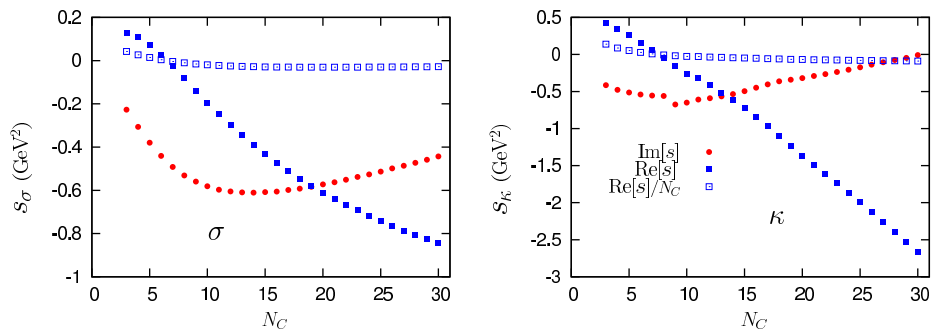**Figure 2:** Masses of resonances as functions of N_C.

Figure 3: N_C trajectories for the imaginary and real parts of σ pole s_σ and κ pole s_κ.

[2] J. R. Peláez, Mod. Phys. Lett. **A19** (2004) 2879; Z. H. Guo, J. J. Sanz-Cillero and H.-Q. Zheng, JHEP **06** (2007) 030; J. Nieves, A. Pich and E. Ruiz Arriola, arXiv: 1107.3247 [hep-ph]; L. Y. Dai, X. G. Wang and H. Q. Zheng, arXiv: 1108.1451 [hep-ph].

[3] J. A. Oller and E. Oset, Phys. Rev. **D60** (1999) 074023; J. A. Oller, Phys. Lett. B **477** (2000) 187; J. A. Oller and U. G. Meissner, Phys. Lett. B **500** (2001) 263.

[4] Zhi-Hui Guo and J. A. Oller, Phys. Rev. **D84** (2011) 034005; Z. H. Guo, J. Prades and J. A. Oller, Nucl. Phys. Proc. Suppl. B **207-208** (2010) 184.

[5] K. Nakamura, *et al.*, (Particle Data Group), J. Phys. G 37 (2010) 075021.